# Spatial frequency, phase, and the contrast of natural images

**Peter J. Bex**

*Institute of Ophthalmology, 11-43 Bath Street, London EC1V 9EL, UK*

**Walter Makous**

*Center for Visual Science, University of Rochester, Rochester, New York 14627*

We examined contrast sensitivity and suprathreshold apparent contrast with natural images. The spatial-frequency components within single octaves of the images were removed (notch filtered), their phases were randomized, or the polarity of the images was inverted. Of Michelson contrast, root-mean-square (RMS) contrast, and band-limited contrast, RMS contrast was the best index of detectability. Negative images had lower apparent contrast than their positives. Contrast detection thresholds showed spatial-frequency-dependent elevation following both notch filtering and phase randomization. The peak of the spatial-frequency tuning function was approximately 0.5–2 cycles per degree (c/deg). Suprathreshold contrast matching functions also showed spatial-frequency-dependent contrast loss for both notch-filtered and phase-randomized images. The peak of the spatial-frequency tuning function was approximately 1–3 c/deg. There was no detectable difference between the effects of phase randomization and notch filtering on contrast sensitivity. We argue that these observations are consistent with changes in the activity within spatial-frequency channels caused by the higher-order phase structure of natural images that is responsible for the presence of edges and specularities.
© 2002 Optical Society of America

OCIS codes: 330.1800, 330.5510, 330.6100, 330.6110, 330.7310, 30.1880.

## 1. INTRODUCTION

The application of linear systems theory to visual processing[1] has led to the widespread use of sine-wave grating patterns in behavioral, electrophysiological, and computational studies of visual perception. However, outside the laboratory the visual system normally processes images of far greater complexity than sine-wave gratings, so the question we address here is how well the understanding derived from gratings generalizes to natural images.

### A. Sine-Wave Gratings
Human sensitivity to sinusoidal modulations in luminance has a classic inverted U shape, peaking at approximately 2–4 cycles per degree (c/deg).[1,2] The drop in sensitivity at higher frequencies has been attributed to blurring from two main sources: the optical limitations of the eye and spatial summation within the visual system.[2] The fall-off in sensitivity at lower spatial frequencies has been attributed to lateral inhibition,[3] spatial summation,[4] and masking by the zero-frequency (dc) components in visual stimuli.[5]

Several authors have also studied the apparent contrast of sinusoidal patterns at suprathreshold contrasts[6–15]; for review see Ref. 16. The general finding of these contrast matching studies has been that at high contrast levels, apparent contrast is relatively independent of spatial frequency, a phenomenon termed "contrast constancy."[9] Contrast constancy has been attributed to spatial-frequency-dependent contrast gain,[9,17,18] or to

noise at low contrasts followed by pseudo-linearity at higher contrasts.[10,11,14]

### B. Natural Images
Natural images have received increasing attention in recent years, and it is becoming clear that there is no simple relationship between experiences of gratings at threshold and the perception of real scenes at high contrast. It has been known for some time that natural images have a characteristic Fourier spectrum[19]:

$$\mathrm{ampl}(f) = cf^{-\alpha}, \tag{1}$$

where amplitude (ampl) is averaged across all orientations, $c$ is a constant, $f$ is spatial frequency, and $\alpha$ represents the negative slope on log-log coordinates. The value of $\alpha$ varies from image to image, but lies within a fairly narrow range (0.7–1.5) in achromatic images[20–25]; see Ref. 26 for a comparison of studies. Several investigators have speculated that the visual system may be specially adapted to exploit this statistical redundancy.[21,22,27–38] For a recent review see Ref. 35.

### C. Contrast in Natural Images
The apparent contrast of broadband images has received relatively little attention; indeed, it has proven difficult even to determine a metric for the contrast of natural images. The conventional metric for sine-wave-grating contrast is Michelson contrast ($C_\mathrm{M}$), which is most commonly calculated as follows:

$$C_M = \frac{L_{\max} - L_{\min}}{L_{\max} + L_{\min}}. \tag{2}$$

While its calculation is simple, $C_M$ is based on the most and the least intense points in the image, irrespective of their surface area, frequency, or relative separation. The root-mean-square (RMS) calculation of image contrast $C_{rms}$ is the standard deviation of luminance values:

$$C_{rms} = \left[ \frac{\sum L_{(x,y)}^2 - \frac{\left(\sum L_{(x,y)}\right)^2}{N}}{N} \right]^{1/2}. \tag{3}$$

This measure is also relatively simple to calculate and is a good predictor of the relative subjective/apparent contrasts of compound grating images[36] and random noise patterns, when divided by the mean luminance of the image.[37] Another contrast metric, band-limited contrast $(C_{bl})$,[38] represents an attempt to take account of the intensity of a point in an image and the local mean luminance at that point by computing a quantity that can be called the local contrast, $C_L$. This is achieved by dividing the luminance $L_b$ of each point in a band-pass-filtered version of the image by the luminance $L_1$ of the corresponding point in a low-pass-filtered version of the image (dividing by zero is avoided by ignoring points with zero denominator) and is therefore more complex to calculate:

$$C_L(x, y) = \frac{L_b(x, y)}{L_1(x, y)}. \tag{4}$$

This produces a matrix of local contrast values (equal in size to the original image), the mean of which is the band-limited contrast of the image:

$$C_{bl} = \overline{C_L(x, y)}. \tag{5}$$

In the present study, we attempt to relate the well-studied perception of grating contrast to the less well-studied perception of natural image contrast. We examine the contribution of structure at particular spatial frequencies to the overall apparent contrast of natural images. A selection of 216 natural images was drawn at random from a calibrated image database.[22] Contrast detection thresholds and suprathreshold apparent contrast matches were obtained following notch filtering (all components within a specific spatial-frequency octave were removed) or phase randomization (the phases of all components within a specific spatial frequency band were randomized). Natural images generally contain edges and specularities and tend to have non-Gaussian-distributed projections. Phase randomization takes any image and turns it into Gaussian-distributed noise of the same power (or, equivalently, variance). The only aspect that is preserved is the variance, with all aspects of the distributions of any projection onto the data such as the mean absolute deviation, or any other moment other than the second, being affected.

## 2. METHODS

### A. Apparatus
Stimuli were generated on a Macintosh G4 computer by using software adapted from the VideoToolbox routines[39] and were displayed on a LaCie Electron22blue monitor at a frame rate of 75 Hz and a mean luminance of 50 cd/m$^2$. The luminance of the display was linearized with pseudo-12-bit resolution[40] in monochrome and calibrated with a Minolta CS-100 photometer. Images were presented in gray scale by amplifying and sending the same 12-bit monochrome signal to all red–green–blue guns of the display. The display measured 36 deg horizontally (1152 pixels), 27.2 deg vertically (870 pixels) and was 57 cm from the observer in a dark room.

### B. Stimuli
The 216 natural images were drawn at random from a calibrated image database as described elsewhere.[22] The source images were imported as 16-bit numbers corresponding to a rectangular image of size 1536 × 1024 pixels. The angular resolution of each image pixel was approximately 2 arc min, and this resolution was maintained in our experiments at the 57-cm viewing distance. Each image was cropped down to the 256 × 256 central square region. The fast Fourier transform (FFT) of the image was calculated with "Numerical Recipes" routines[41] without data windowing. The amplitude of the dc component was set to zero and later was presented at a fixed value (50 cd/m$^2$) to ensure that the mean luminances of all images were equal to one another and to the mean luminance of the background. The 216 images were used to compute some statistical properties of van Hateran's images, but only a subset of ten, described below, were used for the psychophysics tests.

### C. Slope Calculation
The magnitude and phase of each spatial-frequency component were calculated as follows:

$$\mathrm{ampl}_f = (r_f^2 + i_f^2)^{1/2}, \tag{6}$$

$$\rho_f = a\tan(i_f/r_f), \tag{7}$$

where $\rho$ represents the phase and $r$ is the real and $i$, the imaginary part of the complex number for component $f$. The amplitude of each spatial frequency was averaged across orientations. The slope of the function relating log amplitude to spatial frequency was calculated by linear regression.

### D. Spatial-Frequency Filtering
Our 256 × 256 images covered seven octaves (1–128 c/image, 0.125–16 c/deg), following dc adjustment. We used seven single-octave (0.125–0.25; 0.25–0.5; 0.5–01; 1–2; 2–4; 4–8; 8–16 c/deg) spatial-frequency filters that had abrupt ("hatbox") profiles to simplify phase randomization. There were two spatial manipulations:

1. Notch filtering, in which all components within one octave were removed (their amplitude was set to zero).
2. Phase randomization, in which the amplitude of each component was first calculated [according to Eq. (6)] and a new phase for the component was selected at ran-

dom from 0 to $2\pi$ rad.   The new real and imaginary numbers were calculated as follows:

$$r'_f = \mathrm{ampl}_f \times \cos \rho'_f , \qquad (8)$$

$$i'_f = \mathrm{ampl}_f \times \sin \rho'_f , \qquad (9)$$

and they were inserted into the relevant locations of the FFT, preserving Hermitean symmetry.

The inverse FFT was then performed.   The effects of these manipulations on the appearance of the images are shown in Fig. 1.
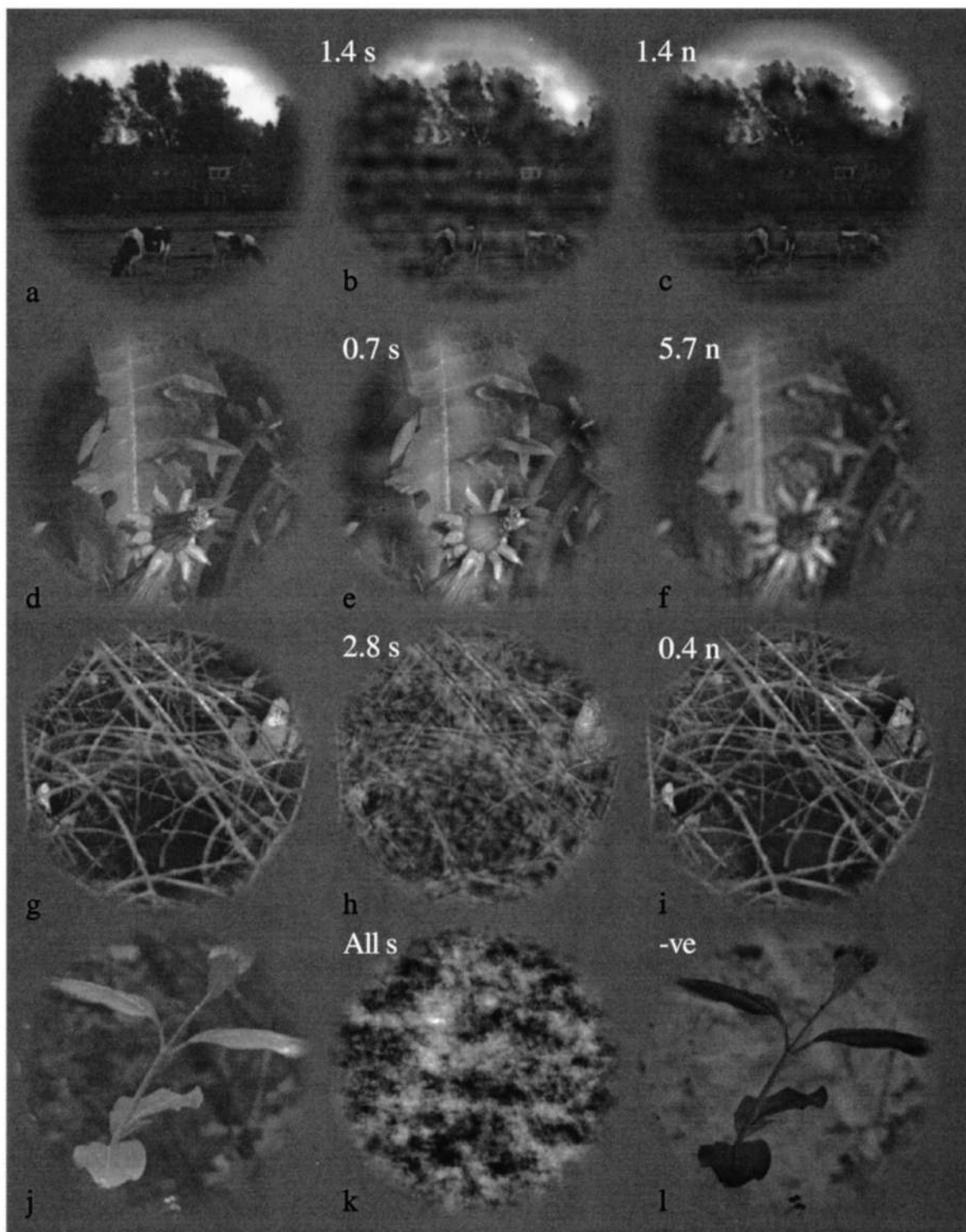


Fig. 1.   Examples of the stimuli.   The images on the left (a, d, g, j) show four images representative of the ten used in the experiments. Each is followed by two versions of the same image after phase randomization (b, e, h, k), notch filtering (c, f, i), or contrast polarity reversal (l).   The center frequency (in cycles per degree) of the one-octave filter is shown in the insets, where relevant (white text).   For image k, the phases of all components were randomized.   See Section 2 for details.

### E.  Contrast Calculations

Removal of the dc component ensured a mean value of zero. The image values were then rescaled so that the mean was 50 cd/m$^2$:

$$L(x, y) = 50 + C_{\mathrm{M}} \times 50 \times \frac{(x, y)}{\max[\mathrm{abs}(x, y)]}.$$

The scaling by $\max[\mathrm{abs}(x, y)]$ confined the range of image values between $-1$ and $+1$ before final scaling (by $C_{\mathrm{M}} \times 50$) to the required luminance range and restoration of the dc component (at 50 cd/m$^2$). $\max[\mathrm{abs}(x, y)]$ was stored and used as a relative contrast metric, denoted scaling contrast, $C_{\mathrm{S}}$. $C_{\mathrm{S}}$ was used to compare the *relative* amplitudes of individual components of a given image, i.e., the amplitude of the individual component following our manipulations of spatial structure (because it was based on the FFT of the same image) relative to its amplitude before the manipulations.

In preserving the mean luminance ($L_{\mathrm{mid}}$) at 50 cd/m$^2$, the actual values of $L_{\mathrm{min}}$ or $L_{\mathrm{max}}$ may be slightly closer to $L_{\mathrm{mid}}$ than expected (because of image specularities). This meant that $C_{\mathrm{M}}$ and $C_{\mathrm{rms}}$ were slightly different from image to image, depending on the spatial frequency of the notch filter and on the particular randomization of phase. Therefore $C_{\mathrm{S}}$, $C_{\mathrm{M}}$ and $C_{\mathrm{rms}}$ were calculated for every image on every trial. The mean value from at least 1280 trials is used in the following data. $C_{\mathrm{bl}}$ was calculated as in Eqs. (4) and (5).[38] For completeness, each of the six single-octave bandpass filters (centered on 0.35, 0.71, 1.41, 2.82, 5.66, or 11.31 c/deg) was used for the analysis (the seventh, centered on 0.18 c/deg, was the lowest octave and had no low-pass image for division).

The images were presented within a circular window 8 deg in diameter, with edges smoothed over 1 deg by a raised cosine. The images were centered 4 deg to the left and right of a central fixation cross. In the threshold task, the images were presented for 500 ms, and the contrast was ramped on and off with a raised cosine temporal envelope lasting 53 ms.

## 3.  PROCEDURE

We selected 10 of the 216 images at random, and examined the effects of two spatial manipulations (notch filtering and phase randomization) in seven bands of one octave each (1–128 c/image). To limit the duration of each run but to distribute observations evenly across conditions, each run examined the effects of one spatial manipulation in one octave, with the ten images randomly interleaved. The resulting 14 conditions (2 spatial-frequency manipulations of 7 frequency bands) were run in random order. We also tested the effects of inverting the polarity of the images.

### A.  Contrast Detection Threshold

The target image (filtered) was presented on the left or right of fixation, at random. The observer was required to indicate its location with a button press. Auditory feedback was provided following incorrect responses. The contrast of the image was under computer control by an independent QUEST staircase[42] for each of the ten interleaved images. Each staircase was initialized with a random contrast and concentrated observations around a contrast level producing 75% correct responses. There were 32 trials for each image on every run, and each run was completed a minimum of 4 times by each observer.

### B.  Contrast Matching

The target image (filtered) was presented on the left or right of fixation, at random, and at a fixed Michelson contrast of 50% (but see Subsection 2.E above). The match image was the unfiltered version (except for dc adjustment and scaling) of the same image. The initial Michelson contrast of the match image was random (1–99%), but during the trial, its contrast was under the control of the observer. The observer was required to adjust the contrast of the match by pressing one of two buttons to increase or decrease the contrast of the match image until a satisfactory contrast match was achieved, indicated by the press of a third button. Observers were required to make at least one adjustment before accepting a match (to preclude acceptance of a random value; if the random starting point happened to match, an increase and a decrease adjustment would be required). There were five matches for each image on every run, and each run was completed a minimum of four times by each observer.

The first stimulus in each row of Fig. 1 is an example of a match stimulus: Its physical contrast was adjusted by the observer so that its apparent contrast matched that of one of the stimuli on the right, depending on whether phase randomization or notch filtering was being tested. In the detection experiments the adaptive program, rather than the observer, made the contrast adjustment to bring the contrast of the image to the threshold for discriminating the image from a homogeneous field.

An additional set of contrast matching data was collected for 100 randomly selected target images whose contrast polarity was inverted. The negative image was presented at a fixed Michelson contrast of 50%. The observer adjusted the contrast of an unfiltered match that was the same image in positive polarity, as before, so that the apparent contrasts of the two images were equal.

## 4.  RESULTS

### A.  Contrast Distributions

Distributions of the contrasts and slopes of the 216 natural images are shown in Fig. 2. Figure 2(a) shows the slopes. These are consistent with previous estimates of the distribution of slopes in natural images, which peak between $-0.7$ to $-1.5$.[20–26] Figures 2(b) and 2(c) show the distributions of Michelson and RMS contrasts, respectively, for an image presented at maximum contrast after dc adjustment and scaling as described above. While $C_{\mathrm{rms}}$ is normally distributed, $C_{\mathrm{M}}$ is positively skewed.

### B.  Contrast Detection

As described in Section 4 above, a random subset of these images was selected for psychophysical analysis. Owing to its unique gray-scale distribution, each image has a unique contrast value for a given luminance range that also depends on the contrast metric employed [including
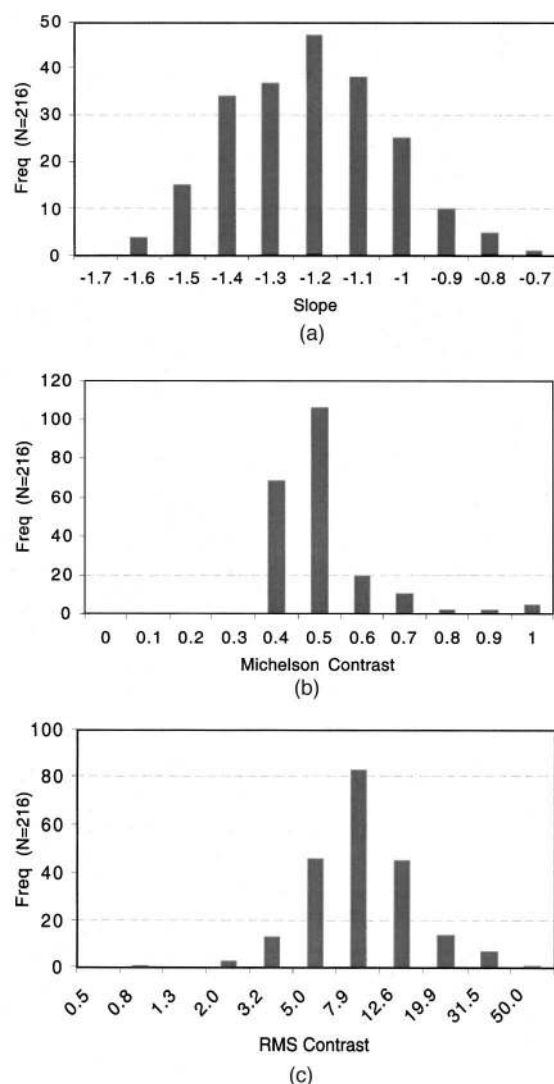
Fig. 2.   (a) Frequency distribution of the slopes of the amplitude spectra of 216 calibrated natural images selected at random from http://hlab.phys.rug.nl/archive.html.   Frequency distribution of (b) the Michelson contrasts and (c) the RMS contrasts of these images, when scaled to maximize contrast.

**Table 1.   Correlation of Observer Sensitivities and Values of Contrast**

| Observer Sensitivities | Correlation Coefficient |
| --- | --- |
| AS versus PB | 0.985 ( $p < 0.001$ ) |
| Mean observers versus $C_M$ | 0.520 ( $p < 0.01$ ) |
| Mean observers versus $C_{rms}$ | 0.925 ( $p < 0.001$ ) |
| Mean observers versus $C_{bl}$ | −0.04 |

$C_M$ because of the dc adjustment; see Subsection 2.B above and Fig. 2(b)].   This means that each contrast metric predicts a different relative threshold for each image. We compared these relative contrasts with those of our observers for $C_M$, $C_{rms}$, and $C_{bl}$.   Table 1 shows the correlation between the contrast sensitivities of the observers and the relative values of $C_M$, $C_{rms}$, and $C_{bl}$ across the images.   Both $C_M$ and $C_{rms}$ were significantly correlated with observers' thresholds, and $C_{rms}$ was signifi-

cantly better than $C_M$ (Fisher's transformation, $z$ = 1.964, $p < 0.05$, two-tailed).   As $C_{bl}$ for a given image differs depending on the passband used to compute it, we show in Table 1 the results for the bandpass octave with peak frequency at 2.82 c/deg, where the contrast sensitivity function peaks for most observers.   However, no matter what passband is used to compute $C_{bl}$, none of the correlations of $C_{bl}$ with contrast sensitivity were significant:   The highest correlation was 0.155, and four of the six correlations were negative.   As we failed to detect any reliable correlation between $C_{bl}$ and contrast sensitivity, and because the value of $C_{bl}$ for images in which the critical passband has been notch filtered is always zero, we did not use the $C_{bl}$ metric in the rest of the experiments.

Figures 3 and 4 show the effects on detection thresholds of notch filtering (squares) all components within a single octave of the image or of randomizing their phases (circles).   Figure 3 shows the data for the author, Fig. 4 for the naïve observers.   The center frequency of the notch filter is shown on the $x$ axis.   Relative threshold contrast, plotted on the $y$ axis, is the threshold contrast
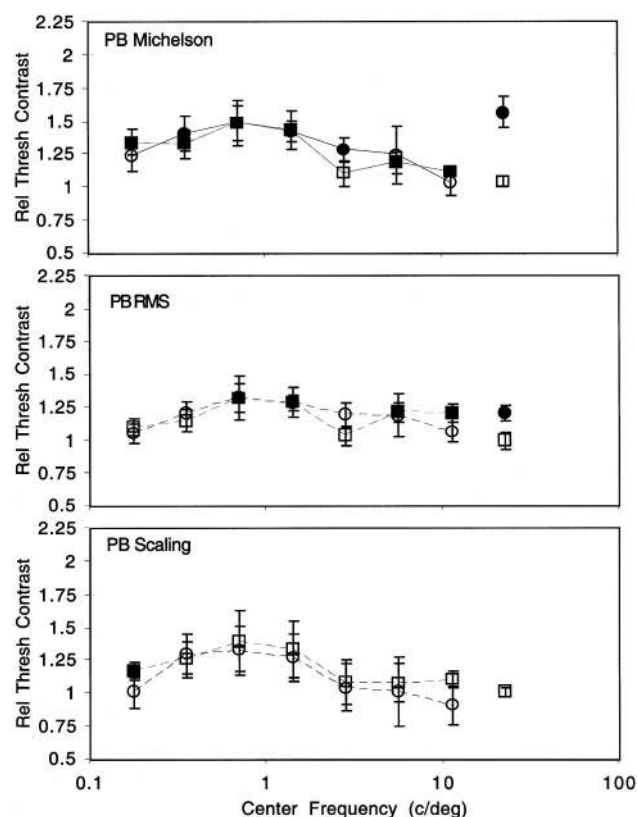


Fig. 3.   Relative contrast detection thresholds for one of the authors (PB).   The data show the detection threshold contrast relative to that for an unfiltered image (dc removed), averaged over the ten images.   Relative contrast is obtained by dividing each threshold by the threshold for the same image without filtering. Squares show relative thresholds for notch filtered images (all components within a single octave were removed); circles show relative thresholds for phase-randomized images (the phases of all components within a single octave were randomized).   The $x$ axis shows the center frequency of the one-octave filter.   Solid symbols indicate data points that are significantly different from unity (i.e., equal threshold contrast).   Error bars show ±1 standard error of the mean. Relative thresholds are shown for Michelson contrast in the upper panel, RMS contrast in the middle panel, and scaling contrast in the lower panel.
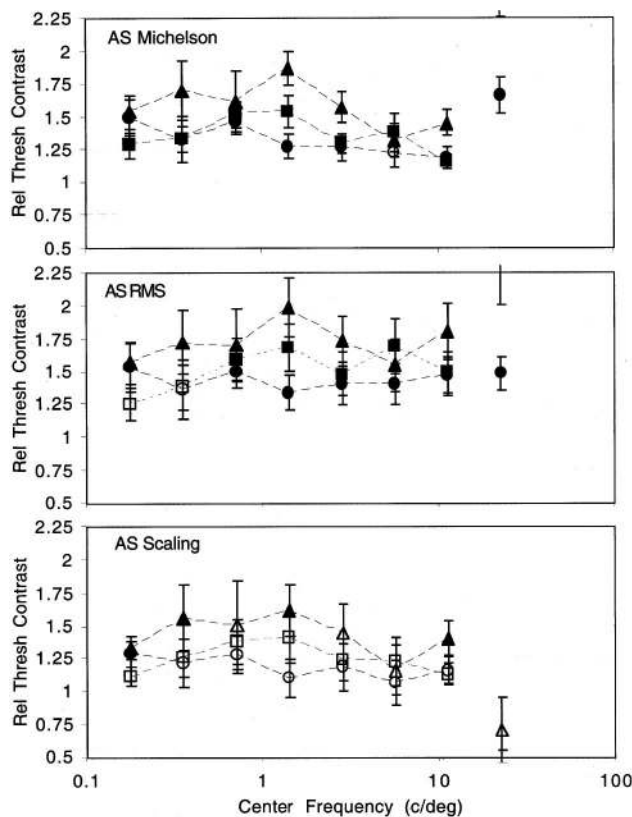
Fig. 4. Same as Fig. 3, for a naïve observer (AS). Triangles show relative thresholds for phase-randomized images for an additional naïve observer.

divided by the threshold for the same stimulus without filtering. An additional set of observations with phase-randomized images is shown for a second naïve observer by the triangles in Fig. 4. The three contrast metrics $C_M$, $C_{rms}$, and $C_S$, are shown in the upper, middle, and lower panels respectively. Each data point shows the mean, and the corresponding brackets show the standard error, of the thresholds for the ten images (none of the images individually deviated significantly from this pattern). The filtered-image thresholds that are significantly different from unfiltered-image thresholds (one sample $t$-test, $p < 0.05$, two-tailed) are identified by solid symbols. The disconnected points at the extreme right of the phase-randomized data (circles) are for images in which the phases of all components were randomized, as in Fig. 1k.

For notch filtering, contrast detection thresholds were generally increased, and the effect was greatest when the components between octaves spanning 0.5–2 c/deg were removed from the image. This pattern was approximately the same for all contrast metrics, with a greater effect manifest in $C_{rms}$. Contrast detection thresholds were also generally increased following phase randomization, even though the images contained the same frequency components. Both observers showed a slight reduction in threshold elevation at higher center frequencies, while only observer PB showed a reduced effect of phase randomization at low frequencies. Because of the difference between observers at low spatial frequencies, we tested a second naïve observer (Fig. 4, tri-

angles), whose detection thresholds, like those of PB, were less affected by phase randomization of low spatial frequencies. The pattern was approximately the same for all contrast metrics, with the greatest effect manifest in $C_M$ and $C_{rms}$.

We were concerned that the lack of effect of high-spatial-frequency structure in our images could be an artifact of local pixel interactions that effectively produce horizontal low-pass filtering of CRT displays,[43] and not a property of the visual system. To address this problem, we collected an additional set of detection thresholds for notch-filtered images that were presented at twice the size and were viewed at twice the distance. In this case, each pixel was doubled horizontally and vertically; otherwise all parameters were as before. The results are plotted as the rightmost data (squares) for PB on Fig. 3 and show that contrast thresholds for unfiltered images and those from which components above 8 c/deg have been removed are not significantly different. This means that local pixel interactions are not responsible for the lack of effect of high-spatial-frequency structure in these images.

### C. Contrast Matching
Figures 5 and 6 show, respectively, the effects on suprathreshold apparent contrast of notch filtering all components within a single octave of the image, or randomizing their phases, for two observers. The data are plotted in the same format as Figs. 3 and 4, except that the $y$ axis shows the match contrast relative to an unfiltered image at a $C_M$ of 50%. Note that the actual value of $C_M$ for the standard image was usually slightly less than this [see Subsection 2.B above and Fig. 2(b)]. To facilitate comparison between the data for contrast matching and contrast detection, we have plotted the inverse of the relative matching contrasts. For both notch-filtered and phase-randomized images, the removal or phase randomization of components in the vicinity of 2–4 c/deg reduced the apparent contrast of the image.

Table 2 shows the relative contrast required to match the contrast of a positive image to that of a negative one, averaged over 100 randomly selected images. The results show that, overall, negative images are slightly but significantly ($t = 5.84$, $p < 0.05$) lower in apparent contrast than positive images. No difference in the apparent contrast of these images is expected from $C_{rms}$. A mean increase (not the decrease we actually observed) of 44% is predicted by $C_M$ because specularities in natural images mean that inverting the contrast polarity tends to reduce the denominators $L_{max}$ and $L_{min}$, with a constant difference in the numerator. $C_{bl}$ can predict an increase or a decrease in apparent contrast, depending on the spatial frequencies of the low-pass and bandpass image selected. For the bandpass octave with peak frequency at 2.82 c/deg, it predicts a mean increase of 92%.

Several previous studies have reported that inverted contrast images are difficult to recognize[44–47]; here we show that their apparent contrast is also affected. Although the mean luminance and the power spectrum of each pair of test and match images were equal, observers found this a remarkably difficult task to perform, and the results were quite variable. We therefore urge caution in interpreting these results.

## 5.  DISCUSSION

Numerous investigations have examined the apparent contrast of spectrally simple sine-wave-grating images. The classic finding is that human observers are most sensitive to sine gratings with a spatial frequency in the vicinity of 2–4 c/deg, but at suprathreshold contrasts, apparent contrast is approximately independent of spatial frequency. We measured the contribution of structure at different spatial frequencies to the threshold and suprathreshold apparent contrast of a random selection of a set of natural images whose spatial-frequency spectrum is complex. The spatial-frequency components within one-octave bands of the images were manipulated either by notch filtering (all components were removed) or phase randomization (the phases of the components were randomized). Contrast sensitivity and apparent contrast above threshold were most affected by manipulations of the spatial structure at 0.5–4 c/deg, and phase randomization had approximately the same effect as notch filtering.
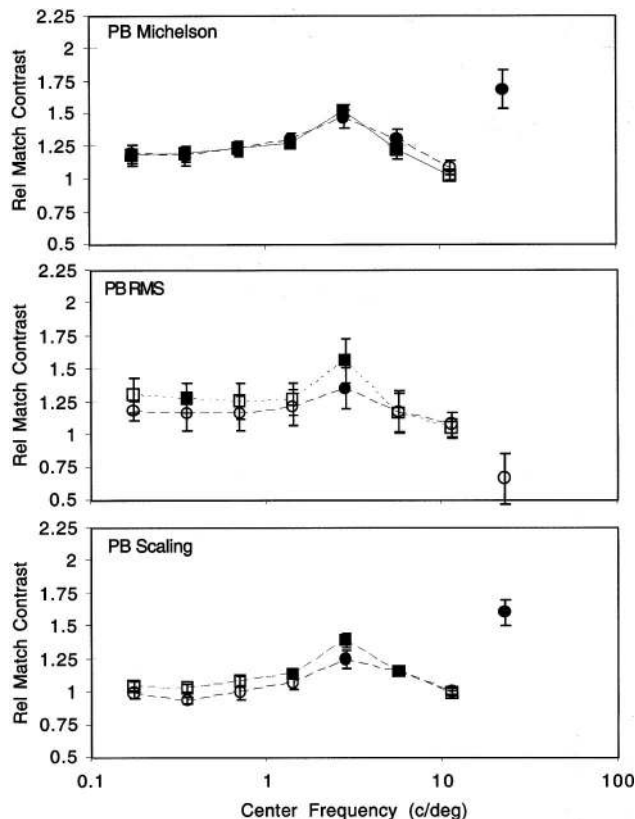


Fig. 5.   Relative contrast matches for one of the authors (PB). The data show the inverse of the relative contrast of an unfiltered image (dc removed) that matched that of a filtered image of 50% Michelson contrast, averaged over the ten images. The inverse facilitates comparison with Figs. 3 and 4. Squares show relative apparent contrast of notch-filtered images; circles show relative apparent contrast of phase-randomized images. The $x$ axis shows the center frequency of the one-octave filter. Solid symbols indicate data points that are significantly different from unity (i.e., equal apparent contrast). Error bars show $\pm 1$ standard error of the mean. Relative apparent contrasts are shown for Michelson contrast in the upper panel, RMS contrast in the middle panel, and scaling contrast in the lower panel.
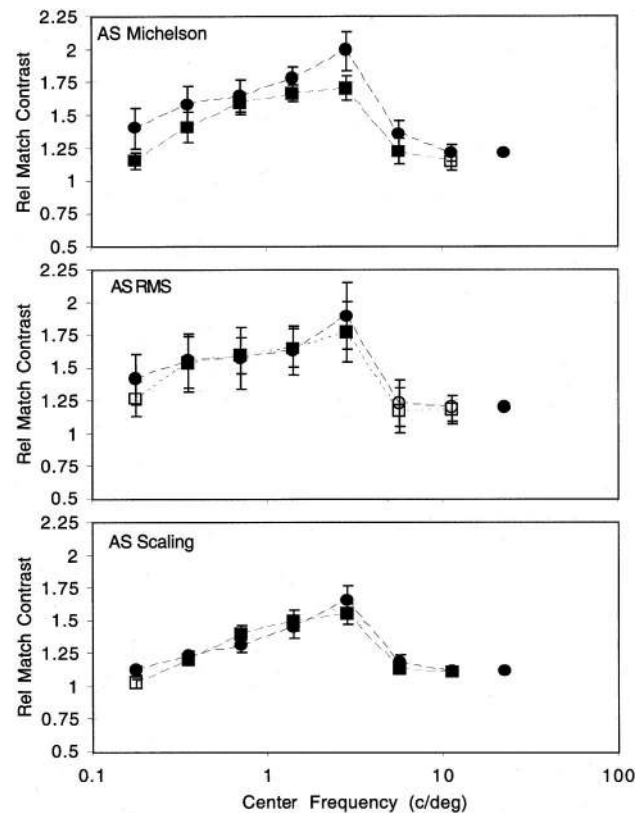


Fig. 6.   Same as Fig. 5, for a naïve observer.

### Table 2.  Comparison of Positive and Negative Image Contrast

| Observer | Mean | Standard Error |
|---|---|---|
| PB | 0.465 | 0.011 |
| AS | 0.468 | 0.016 |
| SD | 0.481 | 0.014 |

### A.  Contrast Metrics

At least three metrics for the contrast of complex images are in common use, as described in Section 1. As part of experiment 1, we collected contrast detection thresholds for ten natural images with a mean luminance fixed at 50 cd/m$^2$. Owing to the unique luminance distributions of these images, each image has a unique contrast for each of the three metrics described here. On the assumption that the image with the highest contrast would be most easily seen, we calculated $C_M$, $C_{rms}$, and $C_{bl}$ for the ten images and compared them with the relative contrast sensitivities of our observers. The best agreement was with $C_{rms}$, and there was no noticeable agreement with $C_{bl}$. Our results therefore support the use of RMS contrast as the most reliable indicator of the visibility of broadband images, in line with previous studies of compound gratings[36] and noise images.[37]

According to channel models of visual processing[1,48,49] any image can be detected when any one of the channels responding to the image exceeds its threshold. As $C_{bl}$, $C_M$, and $C_{rms}$ do not correspond to the responses of channels, but are simply indices of the relative image con-

trasts calculated on a global level, they are difficult to relate to the predictions of channel models.

## B.  Threshold Contrast

The results in Figs. 3 and 4 show that the contrast detection thresholds (by any contrast metric) of natural images are increased by notch filtering and by phase randomization.  The magnitude of the increase depends on the spatial frequencies that are manipulated, peaking at the frequencies to which the visual system is most sensitive for images of this size (1–2 c/deg).[50–54]  It is not surprising that removal of the frequencies to which the visual system is most sensitive raises thresholds, but it may be surprising that the effect of randomizing the phases of those frequencies is just as great as removing them altogether, because randomizing phase has no effect on the amplitude spectrum.  As the excitation of channels in most models depends only on the frequency spectrum within their sensitive band, such models predict that phase randomization would have no effect at all.

$C_s$ is a direct measure of the effects of band filtering or phase randomization on threshold and apparent contrast that does not depend on any particular measure of contrast.  It simply tells how much overall contrast has to be increased to reach threshold or the criterion matching contrast after notch filtering or phase randomization, compared with what it was before the band filtering or phase randomization.  It is not obvious *a priori* that it should correlate with other measures of threshold and apparent contrast, such as $C_M$ or $C_{rms}$.  One might rather expect that $C_M$ would be constant at threshold, but these results show that even after rescaling the contrast to compensate for losses of contrast produced by band filtering or phase randomization, the contrast has to be increased even more to reach threshold or the criterion matching contrast.

It is well established that the relative phase of frequencies that excite separate channels has no effect on thresholds.[49]  To reconcile the effects of phase randomization with the evidence of phase independence, the phase randomization must act through its effects on the frequency components within individual channels.  Others have made the point that there is higher-order structure in natural scenes that produces such features as edges and specular reflections.[35]  Images with the spectrum of natural scenes and random phase lack those features.  Our results show that the visual system is sensitive to the phase structure of natural images, such as the phase structure produced by edges and specular reflections, because disrupting the structure affects both thresholds and apparent contrast (discussed below).

The fact that phase randomization raises thresholds as much as filtering does may be a ceiling effect and therefore misleading.  Once excitation of a channel that participates in detection is reduced significantly below threshold, other channels mediate detection.  Any further reduction in excitation of the first channel has no affect on detection because it is now mediated by another channel.  So phase randomization merely needs to reduce excitation of the most sensitive channel below threshold and need not have as great an effect on that channel as filtering does in order to have equal effects on threshold.

The range of frequencies affected by these manipulations may be broadened beyond the range of individual channels by probability summation among nearly equally excited channels.  Moreover, the range of frequencies affected may also be extended by variation among images, which may bring different channels to threshold in different trials.

## C.  Suprathreshold Contrast

The results of experiment 2 show that the effects of notch filtering and phase randomization on the apparent contrast of natural images are analogous to the effects on sensitivity.  The apparent contrasts (by any metric) of natural images are decreased, the magnitude depending on the spatial frequencies that are manipulated, peaking at the frequencies to which the visual system is most sensitive.  Here again the magnitude of the effect of phase randomization is comparable to that of filtering, although filtering has a slightly greater effect for PB when measured by $C_s$ and $C_{rms}$, and phase randomization has a slightly greater effect for AS when measured by $C_M$.

While the threshold contrast of gratings is highly dependent on spatial frequency, many studies have reported contrast constancy above threshold, where apparent grating contrast is relatively independent of spatial frequency.[6–14]  A leading explanation[9] of contrast constancy attributes it to frequency-specific differences in gain that compensate for frequency-selective attenuation by the optics of the eye.  If the apparent contrasts of all frequencies are equal, zeroing or eliminating the input at different frequencies should have identical effects on apparent contrast, contrary to our findings.  For spatial manipulations between 0.5 and 3 c/deg, the mean relative increase in detection threshold is 1.54 and the mean relative change in suprathreshold apparent contrast is 1.46.  This suggests that for natural images, at least, any frequency-selective differences in gain are too small to compensate entirely for the differences in contrast on the retina, and other explanations must be sought for the difference.

All the studies of contrast matching that show contrast constancy have required subjects to match the contrast of two gratings of obviously different spatial frequency.  Instead, Metha *et al.*[15] recently measured suprathreshold contrast-matching functions for a long series of grating pairs that were not discriminably different in spatial frequency.  Subjects matched the contrast of multiple pairs of gratings that differed in spatial frequency by less than one just-noticeable difference, a procedure that required 40 contrast matches between 1 and 16 c/deg.  The resulting contrast matching functions deviated toward the contrast sensitivity function (inverted U-shaped).  These results suggest that contrast constancy requires discriminable differences in spatial frequency.  Gratings that can be discriminated excite different channels, and the different channels can have different gains that produce equal apparent contrast from unequal retinal contrasts.  Gratings that cannot be discriminated excite the same channel (or the distribution of channel excitation is nearly identical—not discriminably different), so the channels cannot undergo different gains.  The spectrum of natural images is much broader than that of sine-wave

gratings, so the presence or absence of a small number of components cannot effectively modulate the gain in individual channels as may be required to produce contrast constancy.

### D.  Contrast Reversal

Contrast reversal turns a bright spot caused by specular reflection into a dark spot.  If specular reflections are an important cause of differences between natural images and such images as gratings, the lower apparent contrast of negative images implies that dark spots are of less apparent contrast than bright spots.  This implies an expansive luminance nonlinearity.

### E.  Spatial Frequency and Phase

Several studies have examined how the appearance of an image is determined by its phase and amplitude spectrum.[34,55–60]  Exchanging the amplitude or phase spectrum of two images tends to produce a hybrid image that more closely resembles the image that contributed the phase spectrum.  This result is perhaps unsurprising, given the similarity in the amplitude spectra of natural images,[19] and given that full specification of the image of course requires both amplitude and phase.[59,60]  In one-dimensional images, the relative phases of components determine the appearance and location of edges.[61]  Several investigators have reported that observers are sensitive to the relative phases of one-dimensional[62–66] and two-dimensional[67,68] periodic patterns.  Changes in the luminance profile following phase manipulation produce local contrast changes in the image that can account for spatial discrimination without invoking phase-sensitive mechanisms *per se*.[64,65]  Previous studies have concentrated on the high-level global image statistics that support image identification and discrimination.[21,22,31–35]  Although the suprathreshold images used in our matching experiments have sufficiently high contrast to allow analysis of the relative phases across spatial scales, these global image statistics are not available to the observer in our threshold experiments, and yet we still find that phase counts.

These results extend the previous findings of others that image identification and discrimination depend on the phase structure of the image and show that detection and apparent contrast do as well.  Indeed, changing the phase of a component can affect the contrast threshold and perceived contrast of an image as much as removing it altogether.  Our results show that the nonrandom phase structure of natural images, such as those associated with edges, specular reflections, and other features, makes the images more visible and of higher contrast.  Phase randomization destroys this structure as effectively as removal of the components altogether.  This, of course, means not that phase randomization obliterates modulation within the passband but only that it reduces it enough that detection is mediated by the power in other bands.

It is widely accepted that the sensitivity of elements of spatial-frequency channels is somewhat localized in space as well as in spatial frequency.  We suggest that within a given spatial frequency channel, the presence of edges and specularities in natural scenes produces large responses in some areas of the scene, where the in-phase components happen to sum constructively, and weak responses in other parts, where they happen to sum destructively, and that those elements sensitive in the region of summation subserve the detection of threshold stimuli and enhance the apparent contrast of suprathreshold stimuli.  In this way, the occasional convergence of phase in natural scenes may facilitate detection and increase apparent contrast at a local level rather than through global analysis of the higher-order statistics of natural images.

## ACKNOWLEDGMENTS

## REFERENCES

1.  F. W. Campbell and J. G. Robson, "Application of Fourier analysis to the visibility of gratings," J. Physiol. (London) **197**, 551–566 (1968).
2.  F. W. Campbell and D. G. Green, "Optical and retinal factors affecting visual resolution," J. Physiol. (London) **181**, 576–593 (1965).
3.  D. H. Kelly, "Spatial frequency selectivity in the retina," Vision Res. **15**, 665–672 (1975).
4.  J. Hoekstra, D. P. J. Van der Goot, G. Van den Brink, and F. A. Bilsen, "The influence of the number of cycles upon the visual contrast threshold for spatial sine wave patterns," Vision Res. **14**, 365–368 (1974).
5.  J. Yang, X. Qi, and W. Makous, "Zero frequency masking and a model of contrast sensitivity," Vision Res. **35**, 1965–1978 (1995).
6.  O. Bryngdahl, "Characteristics of the visual system:  psychophysical measurements of the response to spatial sinewave stimuli in the photopic region," J. Opt. Soc. Am. **56**, 811–821 (1966).
7.  A. Watanabe, T. Mori, S. Nagata, and K. Hiwatashi, "Spatial sine wave responses of the human visual system," Vision Res. **8**, 1245–1263 (1968).
8.  C. Blakemore, J. P. J. Muncey, and R. M. Ridley, "Stimulus specificity in the human visual system," Vision Res. **13**, 1915–1931 (1973).
9.  M. A. Georgeson and G. D. Sullivan, "Contrast constancy: deblurring in human vision by spatial frequency channels," J. Physiol. (London) **252**, 627–656 (1975).
10.  J. J. Kulikowski, "Effective contrast constancy and linearity of contrast sensation," Vision Res. **16**, 1419–1431 (1976).
11.  M. W. Cannon, Jr., "Contrast sensation:  a linear function of stimulus contrast," Vision Res. **19**, 1045–1052 (1979).
12.  D. O. Bowker, "Suprathreshold spatiotemporal response characteristics of the human visual system," J. Opt. Soc. Am. **73**, 436–440 (1983).
13.  R. St. John, B. Timney, K. E. Armstrong, and A. B. Szpak, "Changes in perceived contrast of suprathreshold gratings as a function of orientation and spatial frequency," Spatial Vision **2**, 223–232 (1987).
14.  N. Brady and D. J. Field, "What's constant in contrast constancy?  The effects of scaling on the perceived contrast of bandpass patterns," Vision Res. **35**, 739–756 (1995).

15. A. B. Metha, P. J. Bex, and W. Makous, "Contrast constancy requires discriminable spatial frequency content," Invest. Ophthalmol. Visual Sci. **39**, Suppl. S424 (1998).

16. M. A. Georgeson, "Over the limit: Encoding contrast above threshold in human vision," in *Limits of Vision*, J. J. Kulikowski, ed. (Erlbaum London, 1990) pp. 106–119.

17. W. H. Swanson, H. R. Wilson, and S. C. Giese, "Contrast matching data predicted from contrast increment thresholds," Vision Res. **24**, 63–75 (1984).

18. W. H. Swanson, M. A. Georgeson, and H. R. Wilson, "Comparison of contrast responses across spatial mechanisms," Vision Res. **28**, 457–459 (1988).

19. E. R. Kretzmer, "Statistics of television signals," Bell Syst. Tech. J. **31**, 751–763 (1952).

20. G. J. Burton and I. R. Moorhead, "Color and spatial structure in natural scenes," Appl. Opt. **26**, 157–170 (1987).

21. D. J. Field, "Relations between the statistics of natural images and the response properties of cortical cells," J. Opt. Soc. Am. A **4**, 2379–2394 (1987).

22. J. H. van Hateren and A. van der Schaaf, "Independent component filters of natural images compared with simple cells in primary visual cortex," Proc. R. Soc. London Ser. B **265**, 359–366 (1998).

23. D. L. Ruderman and W. Bialek, "Statistics of natural images: scaling in the woods," Phys. Rev. Lett. **73**, 814–817 (1994).

24. D. J. Tolhurst, Y. Tadmor, and T. Chao, "Amplitude spectra of natural images," Ophthalmic Physiol. Opt. **12**, 229–232 (1992).

25. A. van der Schaaf and J. H. van Hateren, "Modelling the power spectra of natural images: Statistics and information," Vision Res. **36**, 2759–2770 (1996).

26. V. A. Billock, "Neural acclimation to 1/f spatial frequency spectra in natural images transduced by the human visual system," Physica D **137**, 379–391 (2000).

27. F. Attneave, "Some informational aspects of visual perception," Psychol. Rev. **61**, 183–193 (1954).

28. H. B. Barlow, "Possible principles underlying the transformations of sensory messages," in *Sensory Communication*, W. A. Rosenblith, ed. (MIT Press, Cambridge, Mass. 1961) pp. 217–234.

29. S. B. Laughlin, "A simple coding procedure enhances a neuron's information capacity," Z. Naturforsch. Teil C **36**, 910–912 (1981).

30. M. V. Srinivansan, S. B. Laughlin, and A. Dubs, "Predictive coding: a fresh view of inhibition in the retina," Proc. R. Soc. London Ser. B **216**, 427–459 (1982).

31. J. H. Van Hateren, "Real and optimal neural images in early vision," Nature **360**, 68–70 (1992).

32. C. A. Parraga, T. Troscianko, and D. J. Tolhurst, "The human visual system is optimised for processing the spatial information in natural visual images," Curr. Biol. **10**, 35–38 (2000).

33. D. J. Tolhurst and Y. Tadmor, "Discrimination of spectrally blended natural images: optimisation of the human visual system for encoding natural scenes," Perception **29**, 1087–1100 (2000).

34. M. G. A. Thomson, D. H. Foster, and R. J. Summers, "Human sensitivity to phase perturbations in natural images: a statistical framework," Perception **29**, 1057–1069 (2000).

35. E. P. Simoncelli and B. A. Olshauser, "Natural image statistics and neural representation," Annu. Rev. Neurosci. **24**, 1193–1216 (2001).

36. K. Tiippana, R. Näsänen, and J. Rovamo, "Contrast matching of two-dimensional compound gratings," Vision Res. **34**, 1157–1163 (1994).

37. B. Moulden, F. Kingdom, and L. F. Gatley, "The standard deviation of luminance as a metric for contrast in random-dot images," Perception **19**, 79–101 (1990).

38. E. Peli, "Contrast in complex images," J. Opt. Soc. Am. A **7**, 2032–2040 (1990).

39. D. G. Pelli, "The Videotoolbox software for visual psychophysics: transforming numbers into movies," Spatial Vision **10**, 437–442 (1997).

40. D. G. Pelli and L. Zhang, "Accurate control of contrast on microcomputer displays," Vision Res. **31**, 1337–1350 (1991).

41. W. H. Press, A. A. Teukolsky, W. T. Vetterling, and B. P. Flannery, *Numerical Recipes in C*, 2nd ed. (Cambridge U. Press, Cambridge, UK, 1992).

42. A. B. Watson and D. G. Pelli, "QUEST: A Bayesian adaptive psychometric method," Percept. Psychophys. **33**, 113–120 (1983).

43. A. Naiman and W. Makous, "Spatial non-linearities of gray-scale CRT pixels," in *Human Vision, Visual Processing, and Digital Display III*, B. E. Rogowitz, ed., Proc. SPIE 1666, 41–56 (1992).

44. T. Hayes, M. C. Morrone, and D. C. Burr, "Recognition of positive and negative bandpass-filtered images," Perception **15**, 595–602 (1986).

45. C. H. Liu and A. Chaudhuri, "Are there qualitative differences between face processing in photographic positive and negative?" Perception **27**, 1107–1122 (1998).

46. R. Kemp, G. Pike, P. White, and A. Musselman, "Perception and recognition of normal and negative faces: the role of shape from shading and pigmentation cues," Perception **25**, 37–52 (1996).

47. A. Johnston, H. Hill, and N. Carman, "Recognizing faces: effects of lighting direction, inversion, and brightness reversal," Perception **21**, 365–375 (1992).

48. C. Blakemore and F. W. Campbell, "On the existence of neurones in the human visual system selectively sensitive to the orientation and size of retinal images," J. Physiol. (London) **203**, 237–260 (1969).

49. N. Graham and J. Nachmias, "Detection of grating patterns containing two spatial frequencies: A comparison of single-channel and multiple channel models," Vision Res. **11**, 251–259 (1971).

50. E. R. Howell and R. F. Hess, "The functional area for summation to threshold for sinusoidal gratings," Vision Res. **18**, 369–374 (1978).

51. M. S. Banks, W. S. Geisler, and P. J. Bennett, "The physical limits of grating visibility," Vision Res. **27**, 1915–1924 (1987).

52. J. Mustonen, J. Rovamo, and R. Näsänen, "The effects of grating area and spatial frequency on contrast sensitivity as a function of light level," Vision Res. **33**, 2065–2072 (1993).

53. N. Sekiguchi, D. R. Williams, and D. H. Brainard, "Efficiency in detection of isoluminant and isochromatic interference fringes," J. Opt. Soc. Am. A **10**, 2118–2133 (1993).

54. J. Yang and W. Makous, "Implicit masking constrained by spatial inhomogeneities," Vision Res. **37**, 1917–1927 (1997).

55. A. V. Oppenheim and J. S. Lim, "The importance of phase in signals," Proc. IEEE **69**, 529–541 (1981).

56. L. N. Piotrowski and F. W. Campbell, "A demonstration of the visual importance and flexibility of spatial-frequency amplitude and phase," Perception **11**, 337–46 (1982).

57. J. Bretel, T. Caelli, R. Hilz, and I. Rentschler, "Modelling perceptual distortion: Amplitude and phase transmission in the human visual system," Hum. Neurobiol. **1**, 61–67 (1982).

58. R. Shapley, T. Caelli, S. Grossberg, M. J. Morgan, and I. Rentschler, "Computational thories of visual perception," in *Visual Perception: The Neurophysiological Foundations*, L. Spillman and J. S. Werner, eds. (Academic, New York, 1990), pp. 417–448.

59. M. J. Morgan, J. Ross, and A. Hayes, "The relative importance of local phase and local amplitude in patchwise image-reconstruction," Biol. Cybern. **65**, 113–119 (1991).

60. Y. Tadmor and D. J. Tolhurst, "Both the phase and the amplitude spectrum may determine the appearance of natural images," Vision Res. **33**, 141–145 (1993).

61. M. C. Morrone and D. C. Burr, "Feature detection in human vision: a phase-dependent energy model," Proc. R. Soc. London Ser. B **235**, 221–245 (1988).

62. J. Nachmias and A. Weber, "Discrimination of simple and complex gratings," Vision Res. **15**, 217–223 (1975).

63. D. C. Burr, "Sensitivity to spatial phase," Vision Res. **20**, 391–396 (1980).

64. D. R. Badcock, "Spatial phase or luminance profile discrimination?" Vision Res. **24**, 613–623 (1984).

65. D. R. Badcock, "How do we discriminate relative spatial phase?" Vision Res. **24**, 1847–1857 (1984).

66. M. C. Morrone, D. C. Burr, and D. Spinelli, "Discrimination of spatial phase in central and peripheral vision," Vision Res. **29**, 433–445 (1989).

67. I. Rentschler and B. Treutwein, "Loss of spatial phase rela-

tionships in extrafoveal vision," Nature **313**, 308–310 (1985).

68. P. J. Bennett and M. S. Banks, "Sensitivity loss in odd-symmetric mechanisms and phase anomalies in peripheral vision," Nature **326**, 873–876 (1987).

69. P. J. Bex and W. Makous, "Contrast perception in natural images," Invest. Ophthalmol. Visual Sci. Suppl. **42**, S616 (2001).